General and Comparative Endocrinology 275 (2019) 6–14

Contents lists available at ScienceDirect

General and Comparative Endocrinology

journal homepage: www.elsevier.com/locate/ygcen

The androgenic gland in male morphotypes of the Amazon River prawn *Macrobrachium amazonicum* (Heller, 1862)

Lucas Rezende Penido Paschoal[a,*], Fernando José Zara[a,b]

[a] UNESP – Universidade Estadual Paulista, 13506-900 Rio Claro, SP, Brazil
[b] Invertebrate Morphology Laboratory (IML), Departamento de Biologia Aplicada, CAUNESP and IEAMar, UNESP – Universidade Estadual Paulista, 14884-900 Jaboticabal, SP, Brazil

ARTICLE INFO

Keywords:
Caridea
Histology
Male reproductive system
TEM
Multidisciplinary approach

ABSTRACT

Sexual differentiation and primary and secondary sexual characteristics in male crustaceans are modulated by hormones produced in the androgenic gland (AG). The AG is also responsible for the determination of morphotypes in caridean shrimps, such as *Macrobrachium amazonicum* that shows four morphotypes: translucent claw (TC), cinnamon claw (CC), green claw 1 (GC1) and green claw 2 (GC2). Here, we verified the anatomical, histological and ultrastructural characteristics of the AG in different morphotypes of this species with both amphidromous and hololimnetic life cycles. In submissive morphotypes (TC and CC), the AGs are reduced and concentrated in the terminal expansion of the distal portion of vasa deferentia (DVD), the ejaculatory ducts (ED). In dominant morphotypes (GC1 and GC2) these glands lie along the DVD and ED. Two morphological stages (I and II) were recorded for AG cells. In submissive morphotypes stage I cells predominated in the AGs, while in dominant morphotypes stage II cells were more common. AG cells in both stages were positive for proteins, confirming the protein nature of the secreted hormone. Stage I cells have abundant rough endoplasmic reticulum (RER) with numerous parallel cisternae, whereas in stage II cells, the cisternae of RER are highly dilated. Stage II cells do not produce secretory granules, but they undergo hypertrophy and the hormone release to hemolymph probably occurs by holocrine secretion. The AGs in TC, GC1 and GC2 morphotypes increase as the animals grow and are larger in GC1 males. On the other hand, AGs decrease in the CC morphotype as the animal grows. These differences are related to the type of reproductive strategy adopted by each morphotype. In *M. amazonicum*, the AGs show the same morphological, histochemical and ultrastructural patterns between the different life history populations.

1. Introduction

In numerous species of gonochoric caridean shrimps, sexual dimorphism is clearly evident and is responsible for establishing a social hierarchy in populations. Males of dominant morphotypes with large body proportions and hypertrophied chelipeds have selective advantages over individuals of submissive morphotypes such as territorial dominance, more success at obtaining food resources and greater reproductive success (Ra'anan and Sagi, 1985; Correa and Thiel, 2003; Karplus and Barki, 2018).

The presence of morphotypes in carideans males is common for the genus *Macrobrachium* Spence Bate, 1868: *M. amazonicum* (Heller, 1862) in Moraes-Riodades and Valenti (2004) and Pantaleão et al. (2014), *M. dayanum* (Henderson, 1893) in Langer et al. (2002), *M. idella idella* (Hilgendorf, 1898) in Soundarapandian et al. (2013) and *M. rosenbergii* (De Man, 1879) in Ra'anan and Sagi (1985) and Kuris et al. (1987), and *Rhynchocinetes* H. Milne Edwards, 1837: *R. brucei* Okuno, 1994 in Thiel et al. (2010), *R. durbanensis* Gordon, 1936 in Prakash et al. (2016) and *R. typus* H. Milne Edwards, 1837 in Correa et al. (2003). In all these studies, some common features observed between the dominant morphotypes are the presence of sexual weapons (enlarged, modified and robust second pair of pereiopods, i.e. chelipeds), investment in somatic growth (large sizes), aggressiveness and agonistic interactions (fights) in territorial and reproductive behavior.

Sex differentiation and development of primary (spermatogenesis) and secondary sexual characteristics (masculinization/hypertrophy of the chelipeds) in male crustaceans are regulated by the androgenic glands (AGs) (Charniaux-Cotton, 1954, 1958; Ventura et al., 2011a). In caridean shrimps, AGs are arranged perpendicularly to the distal portion of vasa deferentia and are anatomically easy to identify (Sagi et al.,

* Corresponding author.
E-mail addresses: lucasrezende20@gmail.com (L.R.P. Paschoal), fjzara@fcav.unesp.br (F. José Zara).

https://doi.org/10.1016/j.ygcen.2019.01.014
Received 29 September 2018; Received in revised form 24 January 2019; Accepted 29 January 2019
Available online 30 January 2019
0016-6480/

1997; Bortolini and Bauer, 2016; Paschoal and Zara, 2018, 2019). The most striking ultrastructural characteristic of the AG cells is the large amount of rough endoplasmic reticulum (RER) and electron-dense bodies identified as lysosomes (King, 1964; Radu and Crăciun, 1976). The AG produces an insulin-like peptide hormone (IAG), responsible for crustacean masculinization (Ventura and Sagi, 2012). This hormone is responsible for regulating spermatogenesis, development of gonopores and hypertrophy of chelipeds, determination of morphotypes and modulation of the aggressive behavior in dominant morphotypes (Nagamine et al., 1980a,b; Okumura and Hara, 2004; Ventura et al., 2011a). Nagamine et al. (1980a) and Sagi et al. (1995) demonstrated the regulatory role of AG in *M. rosenbergii* when performing andrectomy (ablation of the AG) in male prawns of this species, promoting the feminization of the individuals after this process.

The Amazon River prawn *M. amazonicum* is a widely distributed species in the Americas (Costa Rica to Argentina – Pileggi et al., 2013) with great potential for world aquaculture (New, 2005), and is highly consumed in the northern and northeastern Brazil (Maciel and Valenti, 2009). This species shows populations with amphidromous (i.e. larvae depend on estuarine water for their development) and hololimnetic (i.e. prawns with an entirely freshwater life cycle) life histories, which confers a wide plasticity of habitat use (estuaries to freshwater lakes) by their phenotypes (Pileggi et al., 2013; Paschoal and Zara, 2018, 2019). Currently, only the amphidromous populations are farmed, and are the most studied for harvesting, management and production (see Moraes-Valenti and Valenti, 2010 for further details). Regardless of the life history adopted, four morphotypes have been described for male prawns of *M. amazonicum* in the majority of populations studied: translucent claw (TC) and cinnamon claw (CC) both considered submissive, and green claw 1 (GC1) and green claw 2 (GC2), which show dominant behavior (Moraes-Riodades and Valenti, 2004; Pantaleão et al., 2014; Paschoal and Zara, 2017, 2018, 2019). The main characteristic features of each morphotype and the differences among the four morphotypes were summarized at Table 1.

Despite the importance of the AG for the development and behavior of individuals in populations, as well as their influence on population structure (e.g. sex and morphotype ratios) (Sagi and Aflalo, 2005; Ventura et al., 2011a; Bortolini and Bauer, 2016), this gland has never been studied in the Amazon River prawn. The knowledge of the anatomical, histological and ultrastructural aspects of AG, as well as the sexual manipulation in caridean shrimps is focused on giant river prawn *M. rosenbergii* (see Nagamine et al., 1980a,b; Sagi et al., 1990, 1995, 1997; Okumura and Hara, 2004; Phoungpetchara et al., 2011; Ventura et al., 2011a,b; Ventura and Sagi, 2012 and others). In this context, we described and compared the histological, histochemical, ultrastructural and morphometric patterns of the AGs in different morphotypes of *M. amazonicum* using animals from amphidromous and hololimnetic populations.

2. Materials and methods

2.1. Animals

Males of *M. amazonicum* with hololimnetic development were collected from the Grande River (20° 30′ 53.6″ S, 46° 50′ 16.4″W) during October 2014 to December 2015. The sampling site is located in the reservoir of the Hydroelectric Power Station of Marechal Mascarenhas de Morais, municipality of Cássia, Minas Gerais state (southeastern Brazil). Wild prawns were captured by passive collection, using six traps (85 cm in length X 35 cm in width/height) baited with small pieces of beef liver. These traps were placed near the margin (0.5–2 m) and removed after four hours. Amphidromous male prawns were obtained from the Crustacean sector of the Aquaculture Center of UNESP/Jaboticabal (CAUNESP – Jaboticabal/SP), during August 2015 to April 2016. This farmed population originally belongs to the estuarine areas of the municipality of Santa Bárbara do Pará, Pará state (northern Brazil) (Paschoal and Zara, 2018).

The hololimnetic and amphidromous males were separated into four morphotypes based on the size and color of the chelipeds, angles of the spines on the carpus and propodus and the pubescence on dactyls, in: translucent claw (TC), cinnamon claw (CC), green claw 1 (GC1) and green claw 2 (GC2), according to Moraes-Riodades and Valenti (2004) and Pantaleão et al. (2014). Subsequently, prawns had carapace length (CL), total length (TL), major cheliped length (MCL) and *appendix*

Table 1
Schematic comparison of the main characteristics (ecological, morphometric, behavioral and physiological) of the four male morphotypes of *M. amazonicum*. CC: cinnamon claw; CL: carapace length; GC1: green claw 1; GC2: green claw 2; TC: translucid claw.

Characters	Morphotypes			
	TC	CC	GC1	GC2
1. Proportion in populations[1–3]	high	medium – low	low – very low	low – very low
2. Body size[1–5]	small	medium	large	large
3. Mass gain[6]	high	high	high	low
4. Cheliped color[1,4] (Pantone® – GP1401)[3]	translucent (no code)	beige – greenish beige (451C, 4505 and 466C/U)	moss green (7733-7736C/U)	moss green (2266, 3308 and 560-562C/U)
5. Cheliped size – MCL[1–5]	small	medium	large	very large
6. Allometry: CL *vs.* MCL[1,2]	negative	negative	positive	negative
7. Mating behaviour[2–4,6]	submissive	submissive	(sub)dominant	dominant
8. Mobility[2–4,6]	highly active	highly active	active	sedentary
9. Concentration of spermatozoa in testes[2,3,5,7]	medium	low – absent	high	high
10. Sperm count[3,8]	high	reduced	high	high
11. Androgenic gland size – AG[7,9]	reduced	reduced	large	large
12. Allometry: AG *vs.* CL[9]	negative	eniantometric	negative	negative

[1]Pantaleão et al. (2014).
[2]Paschoal and Zara (2019).
[3]Paschoal (2017).
[4]Moraes-Riodades and Valenti (2004)
[5]Silva et al. (2009).
[6]Augusto and Valenti (2016).
[7]Papa (2007).
[8]Paschoal and Zara (2018).
[9]Present study.

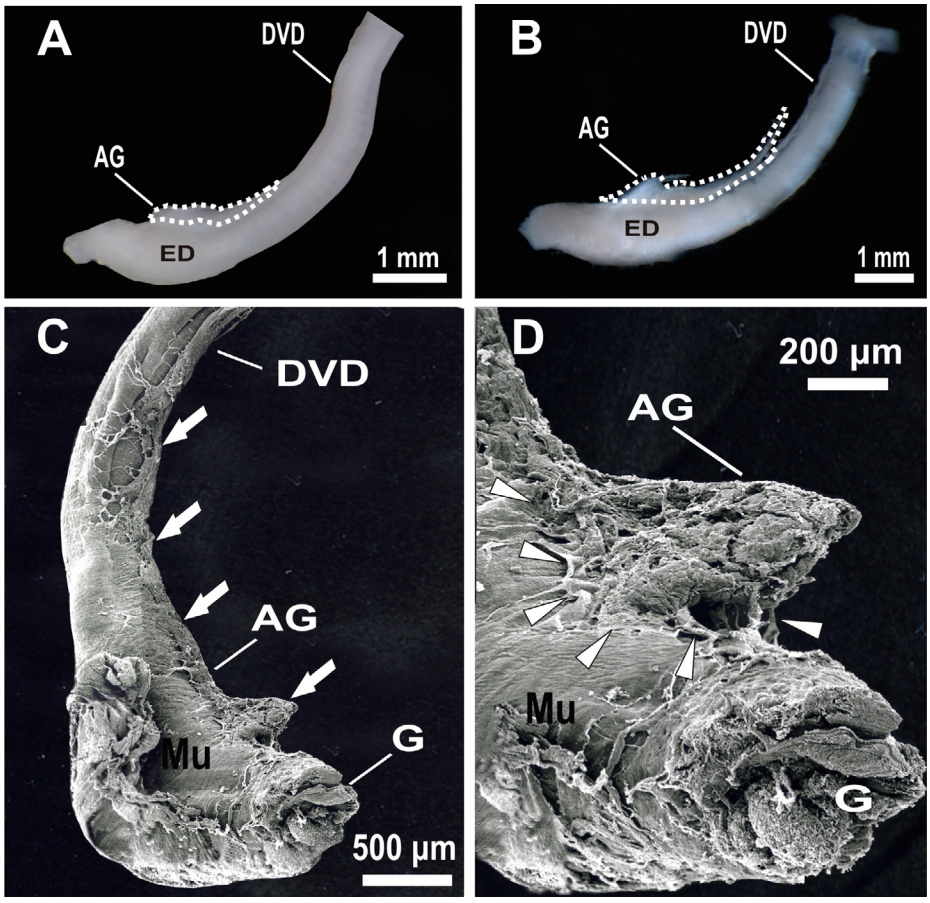

Fig. 1. A and B. Distal portion of vas deferens of *M. amazonicum* males of morphotypes TC and GC2, respectively, showing the androgenic gland arranged parallel to the vas deferens. The dotted lines show the delimitation of the androgenic gland areas. C. Androgenic gland in GC1 morphotype. In dominant males, this structure spreads over the distal portion of vas deferens (white arrows). D. The androgenic gland is attached to the muscle tissue of the vas deferens by connective tissue (white arrowheads). AG: androgenic gland; DVD: distal portion of vas deferens; ED: ejaculatory duct; G: genital pore; Mu: muscle layer.

masculina length (AML) measured with an analogic caliper (0.02 mm), according to Paschoal and Zara (2019). The fresh weight (W) of each individual was obtained with an analytical scale (± 0.0001 g).

2.2. Histology, histochemistry and cell measurements

For anatomical and histological analyzes, 40 individuals (five animals of each morphotype per population) were anesthetized by chilling (− 20 °C/5 min.) and dissected. The distal portion of vas deferens (DVD) with AGs was fixed in 4% paraformaldehyde in 0.2 M sodium phosphate buffer (pH 7.2) for 24 h (4 °C). Subsequently, they were washed twice in the same buffer, dehydrated in an increasing series of ethanol (70–95%), and embedded and included in glycol-methacrylate historesin Leica®. Sections of 4–5 µm were obtained in rotary microtome and the slides were stained with hematoxylin and eosin (H&E), according to Junqueira and Junqueira (1983). For histochemical analyzes, the slides were stained with xylidine ponceau for total proteins (Mello and Vidal, 1980), Alcian blue (pH 1 and 2.5) and periodic acid of Schiff (PAS) for acid and neutral polysaccharides, respectively (Pearse, 1960; Junqueira and Junqueira, 1983). For lipids, the samples were directly embedded and included in historesin after the fixation, avoiding the dehydration (Zara et al., 2012). Subsequently, slides were stained with Sudan black B (Junqueira and Junqueira, 1983).

The nucleus: cytoplasm (N/C) ratio of the AG cells was calculated according to the formula: N/C = (nucleus area/cell area) X 100. The cell areas were obtained by manual delimitation of the nucleus and the entire cell with the software Leica® IM50, measured using a 20X objective on slides stained with H&E. For each morphotype, slides of at least three males were examined (N: 45 cells per morphotype). The N/C ratios of the morphotypes AG cells were tested for normality using Shapiro-Wilk test (normality satisfied – W-Statistic = 0.98, *p*: 0.09). Subsequently, an analysis of variance (ANOVA) with Tukey post-hoc comparisons test (α: 0.05) was used to verify differences between the N/C ratios of the AG cells in morphotypes.

2.3. Electron microscopy

For transmission electron microscopy (TEM), AGs samples ($\leq 1\ mm^3$) were fixed in 2.5% glutaraldehyde in 0.08 M sodium cacodylate buffer (pH 7.2) for four hours at 4 °C, washed and post-fixed in 1% osmium tetroxide in the same buffer (4 °C) for two hours. The samples were "Enbloc" stained with 1% aqueous uranyl acetate (overnight at 4 °C) and dehydrated in an ascending series of acetone (70–100%), embedded and included in Epon-Araldite® resin. Ultrathin sections were obtained in ultramicrotome Leica® UC7 and the grids were stained with 2% aqueous uranyl acetate and 0.4% lead citrate. All grids were examined and photographed using a Jeol J1010 TEM operated at 80 kV.

For scanning electron microscopy (SEM), the DVDs were fixed and post-fixed using the same TEM protocol. The samples were dehydrated in ethanol series (70–100%), completely dried at critical-point EMS 850, attached on stubs and sputter-coated with gold in Denton vacuum desk II sputtering. The AGs were observed and photographed in a Jeol-JSM 5410 SEM, at 10–20 kV.

2.4. Measurement of androgenic gland

In order to avoid that external factors (e.g. temperature, nutrition and seasonality) affected the activity and, consequently, the size of the AGs in morphotypes (Okumura and Hara, 2004), only individuals of the farmed population had their glands measured. Ten amphidromous males of each morphotype (N: 40) were anesthetized by chilling and had their reproductive systems carefully removed. Subsequently, the vasa deferentia (VD) were separated from the testes of animals, had

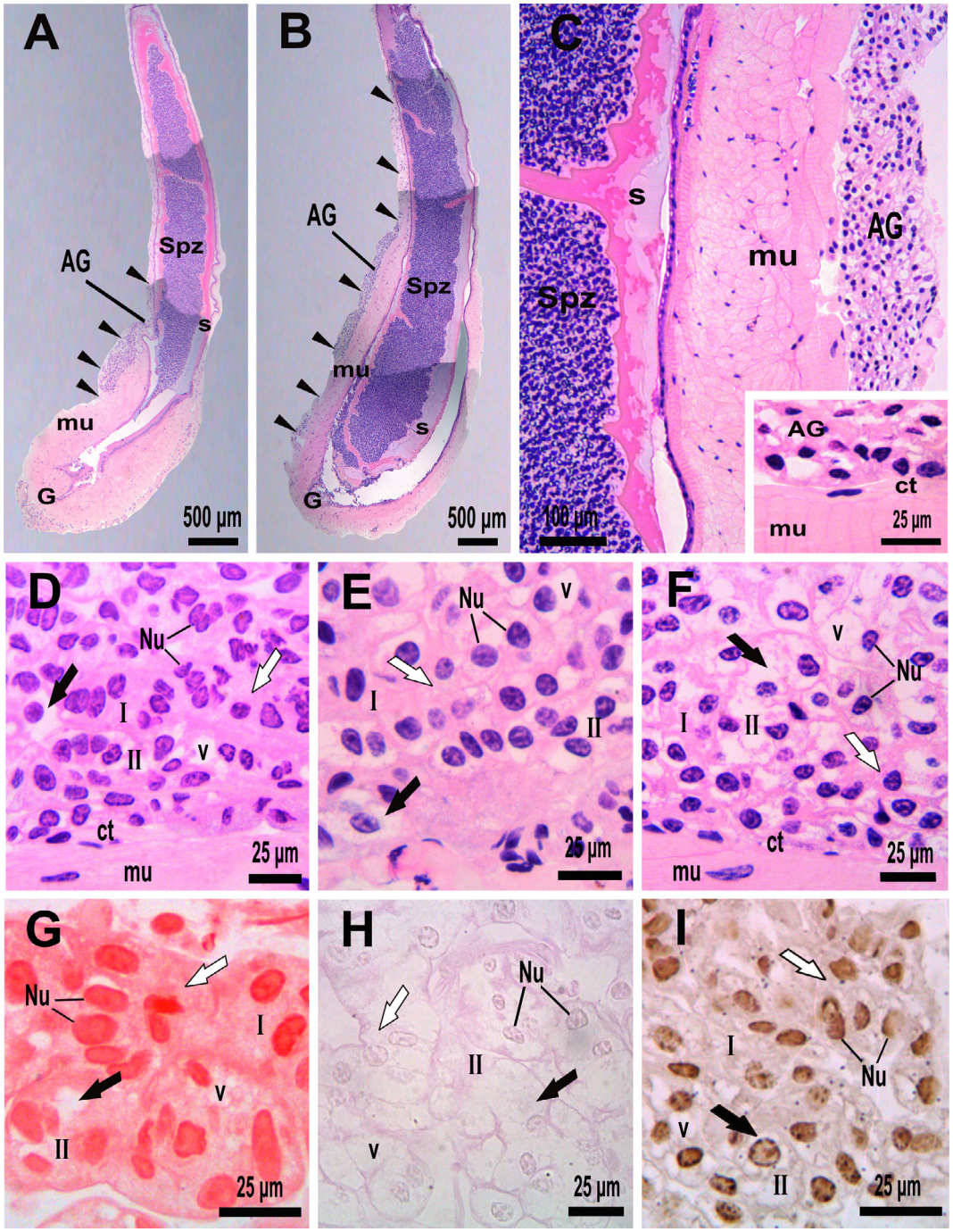

Fig. 2. A. Distal portion of vas deferens in *M. amazonicum* male morphotype TC showing a small androgenic gland concentrated in the bulb of the ejaculatory duct (black arrowheads) [H&E]. B. Distal portion of vas deferens of a GC1 male with androgenic gland occupying a large area of this structure (black arrowheads) [H&E]. C. Androgenic gland attached to the thick muscle layer of the distal portion of vas deferens by a thin layer of connective tissue [H&E]. D. In morphotype TC, the majority of androgenic gland cells are in stage I. These cells are compacted, with large nuclei and no vacuoles in the cytoplasm [H&E]. E. Androgenic gland in CC males show similar proportion of cells in stages I and II [H&E]. F. GC2 males show a high proportion of androgenic gland cells in stage II, with large vacuoles [H&E]. G. Positive reaction for proteins in androgenic gland cells [xylidine ponceau]. H and I. Androgenic gland cells are negative to neutral polysaccharides and lipid techniques [PAS and Sudan black B, respectively]. Note in all morphotypes, accumulation (white arrows) and secretion (black arrows) of hormone in the cytoplasm of these cells. I: stage I cells; II: stage II cells; AG: androgenic gland; ct: connective tissue; G: genital pore; mu: muscle layer; Nu: nucleus; s: secretion; Spz: spermatozoa; v: vacuole.

their ejaculatory ducts (ED) measured, and were maintained in 4% paraformaldehyde. The AGs were measured under a Leica® stereomicroscope by manual delimitation, drawing a line surrounding the glands on the VD and ED (Fig. 1A-B). The AG areas were recorded using the software Leica® IM50, with appropriate calibration for the objective lens used.

Since no statistical differences in the measurements were found between the AGs areas of the left (l) and right (r) side of the same individual (*t*-test = N: 40 – $t = 0.04$, p: 0.96), we used the mean value obtained by measuring both glands of each prawn ($\bar{X} = (l + r) / 2$) for comparison among morphotypes, avoiding pseudoreplication. The differences between the AG areas in morphotypes were tested with

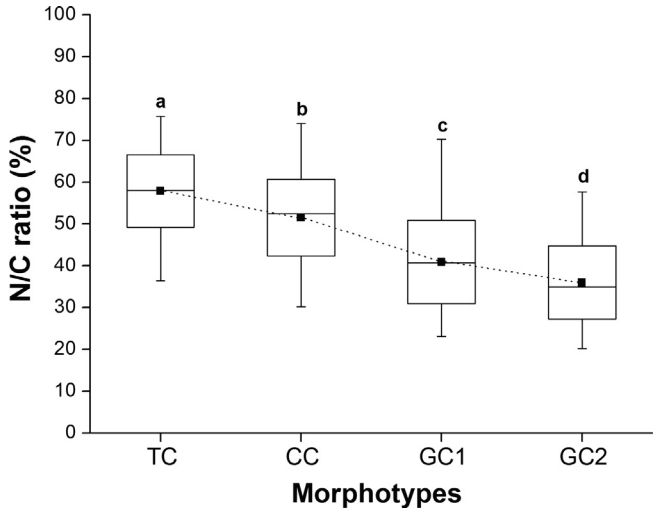

Fig. 3. Nucleus: cytoplasm (N/C) ratio of androgenic gland cells for male morphotypes of *M. amazonicum*. Minimum, maximum (whiskers), mean (black squares) and standard deviation (boxes) values were plotted for each morphotype. Different letters are significantly different in pairwise comparisons. CC: cinnamon claw morphotype; GC1: green claw 1 morphotype; GC2: green claw 2 morphotype; TC: translucid claw morphotype.

ANOVA followed by a Tukey test (α: 0.05), since the data had a normal distribution (W-Statistic = 0.96, *p*: 0.13). Linear regressions were adjusted, having as independent variables (X) the CL, TL and MCL and related them to the AG area (Y – dependent variable) in each morphotype and for all grouped males. The coefficients of determination (r^2) and slopes (*b* – verified by the Student's *t*-test) of the regression lines were calculated, in order to verify the growth pattern of AGs in *M. amazonicum* morphotypes (Gotelli and Ellison, 2004). The *b* of the regressions is the allometric constant that expresses the relation between two variables. If $b > 2$ is characterized a positive allometric growth (Y grows at a higher scale than X), if $b < 2$ the growth is negative allometric (Y grows at a lesser scale than X), and when $b = 2$ is considered as isometric (Y and X grows proportionally) (Gould, 1966). If *b* has a negative value, eniantometry occurs, where the dependent variable decreases in size with body growth (Teissier, 1960). All calculations and statistical analyzes were performed with the software R version 3.3.1. (R Development Core Team, 2016).

3. Results

The androgenic glands in males of *M. amazonicum* are arranged longitudinally over the dorso-medial surface of the muscle layer of the DVD (Figs. 1A-C and 2A-B). These structures show anatomical differences among morphotypes, with similar patterns of arrangement and distribution among the populations analyzed. In TC and CC morphotypes, the AGs show small sizes and are usually concentrated in the terminal expansion of the DVD, the bulbs of the EDs (Figs. 1A and 2A). In GC1 and GC2 morphotypes, the AGs extend from the DVD and spread over the bulbs of the EDs (Figs. 1B-C and 2B). The AGs are always disposed to the ventral surface of the VD on a thin layer of connective tissue, which is attached to a thick musculature of the DVD (Figs. 1C-D and 2C).

The AG cells can be classified according to the degree of cytoplasmic vacuolization, indicating two distinct morphological stages of secretory activity in these cells: I or initial and II or final (Fig. 2D-I). We also observed a reduction in the N/C ratio of the AG cells along the sequential development of morphotypes ($F = 53.05$, $p < 0.001$ – Tukey = TC-CC: 3.28, CC-GC1: 5.50, and GC1-GC2: 2.55, $p < 0.001$) (Fig. 3). Stage I cells are predominant in the AGs of the initial morphotype TC. At this stage, the cells have a larger nucleus in relation to the cytoplasm (N/C: 57.8 ± 8.7%), which has no vacuoles, and only a few cells are at stage II. In general, AG cells in this morphotype are well attached to each other, producing a more compact appearance (Fig. 2D). In the intermediate morphotype CC, stage I and II cells show similar numerical proportion. However, they show a smaller N/C ratio (51.5 ± 9.2%) when compared to TC morphotype AG cells (Fig. 2E). The histology of the AG in GC1 and GC2 morphotypes are quite similar. In these morphotypes, stage II cells are more abundant and swollen than stage I cells, which is less frequent. Stage II cells are characterized by large vacuoles, empty areas and/or unstained cytoplasm (Fig. 2F), showing a higher cytoplasmic content when compared to the submissive morphotypes AG cells (N/C: 40.9 ± 10.0% and 35.9 ± 8.8% for GC1 and GC2, respectively). Despite the differences in histological patterns (stages), no histochemical differences were detected in the AGs among the four morphotypes or the individuals of populations. The cytoplasm and nucleus of the AG cells were positive for proteins (Fig. 2G) and negative for acid (not shown here) and neutral polysaccharides (Fig. 2H), and lipids (Fig. 2I) as well.

Under TEM, the AG is surrounded by a thin conjunctive sheath and both cell types show the cytoplasm filled by the rough endoplasmic reticulum (RER) (Fig. 4A). Stage I cells show the cytoplasm nearly completely filled by RER with parallel lamella or cisternae, and between this organelle it is possible to observe mitochondria and Golgi complexes. Among of the RER with the Golgi complex is frequently observed many vesicles (Fig. 4B). An electron-dense material is also observed inside of the RER (Fig. 4C). In the cytoplasm, electron-dense bodies of variable sizes (approximately 3 μm), spheroidal in shape and limited by single membranes that resemble lysosomes are also found (Fig. 4D-E). Stage II cells show cytoplasm with RER presenting highly dilated cisternae filled with a thin granular material forming vacuoles. These vacuoles displace the cellular organelles which is the main feature of this stage. In addition, degenerate mitochondria showing a few cristae are commonly observed in the cytoplasm of these swollen cells (Fig. 4F-G).

We observed a gradual increase of body size, weight and length of chelipeds in *M. amazonicum* during the passage from one morphotype to another (Tables 1 and 2). The areas of the AGs differed throughout the development of morphotypes ($F = 17.08$, $p < 0.001$). In the initial morphotype TC, the AG area was 0.69 ± 0.18 mm^2, a higher value than that recorded for the intermediate morphotype CC with 0.62 ± 0.14 mm^2. Despite the body size increment observed in CC males, the AG area did not show significant differences between these morphotypes (Tukey = 0.71, *p*: 0.48). When passing to the morphotype GC1, a significant increase of the AG area occurs (Tukey = 5.76, $p < 0.001$), with a subsequent stabilization of the growth of this structure when becoming GC2 males (Tukey = 0.84, p: 0.41). In dominant morphotypes, the AG area was 1.15 ± 0.26 mm^2 in GC1 and 1.07 ± 0.21 mm^2 in GC2.

The comparative analysis of the AG areas in relation to the morphometric variables showed that in males of *M. amazonicum* (pooled data) these structures increased as the animals grew (negative allometry), but when analyzed separately the morphotypes showed distinct characteristics (Table 3 and Fig. 5). Morphotypes TC, GC1 and GC2 presented negative allometric growth for the relationship AG area *vs.* CL, TL and MCL, with morphotype GC1 showing great variability in AG size and higher mean values of AG area when compared to the other morphotypes. On the other hand, in CC morphotype the AG area decreases as the individual grows, i.e. eniantometry (*sensu* Teissier, 1960) (Table 3 and Fig. 5).

4. Discussion

The androgenic glands in *M. amazonicum* are arranged with the typical pattern described in other caridean shrimps, gonochoric or protandric simultaneous hermaphrodites (Hoffman, 1969; Okumura and Hara, 2004; Phoungpetchara et al., 2011; Bortolini and Bauer,

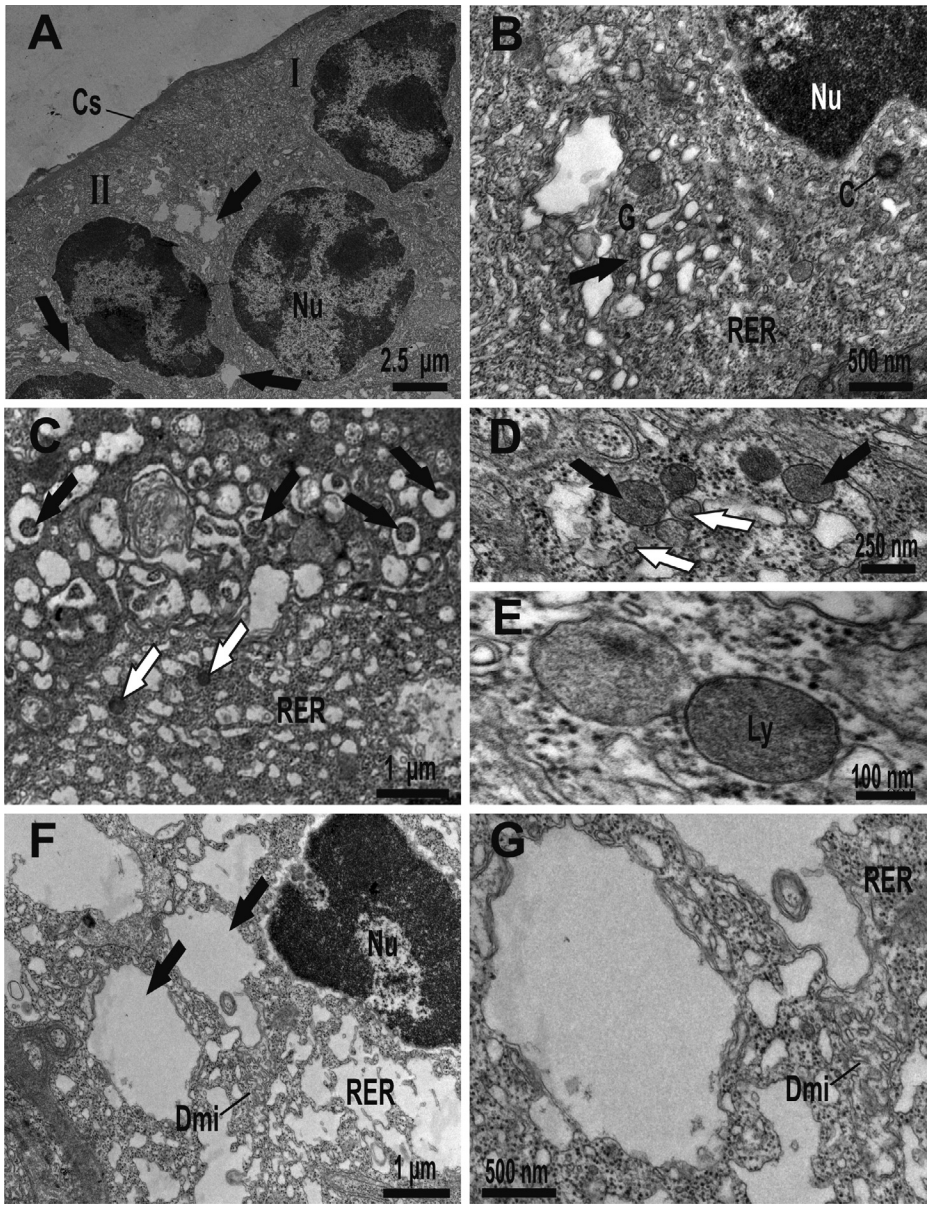

Fig. 4. A. Androgenic gland cells in different stages. Stage I cells show cytoplasm without vacuoles, which characterizes stage II cytoplasm (black arrows). B. Stage I cells have RER with numerous cisternae in the cytoplasm. Note that the Golgi complex has small electron-dense vesicles (black arrow). C. Formation (white arrows) and condensation (black arrows) of electron-dense bodies in the RER cisternae. D. Electron-dense bodies show variation in electron-density and size (black and white arrows). E. Electron-dense bodies identified as lysosomes are surrounded by one membrane. F. Stage II cells showing RER with highly dilated cisternae (black arrows) and degenerate mitochondria in their cytoplasm. G. Detail in higher magnification of F, showing a dilated cisterna of RER with granular material in its interior. I: stage I cells; II: stage II cells; C: centriole; Cs: conjunctive sheath; Dmi: degenerate mitochondria; G: Golgi complex; Ly: lysosome; Nu: nucleus; RER: rough endoplasmic reticulum.

Table 2
Mean (± standard deviation) values of the analyzed morphometric variables, weight and sexual characters in morphotypes of *M. amazonicum* in populations with distinct life histories. A: amphidromous; AML: *appendix masculina* lenght; CC: cinnamon claw; CL: carapace length; ED: ejaculatory duct length; GC1: green claw 1; GC2: green claw 2; H: hololimnetic; MCL: major cheliped length; TC: translucid claw; TL: total length; W: fresh weight.

Morphotypes	Life history	CL (mm)	TL (mm)	MCL (mm)	W (g)	AML (mm)	ED (mm)
TC	A	13.33 ± 2.71	46.27 ± 8.31	24.27 ± 3.76	1.7896 ± 0.8778	3.96 ± 0.62	2.40 ± 0.46
CC	A	17.17 ± 1.37	57.61 ± 3.76	32.71 ± 3.39	3.1970 ± 0.7897	4.67 ± 0.38	2.98 ± 0.28
GC1	A	21.72 ± 0.90	68.68 ± 4.22	56.22 ± 11.84	5.9885 ± 0.8924	5.85 ± 0.26	3.46 ± 0.27
GC2	A	26.25 ± 2.10	79.00 ± 5.50	98.55 ± 15.51	9.8632 ± 1.8928	6.74 ± 0.51	3.64 ± 0.37
TC	H	10.39 ± 2.15	37.15 ± 7.02	19.67 ± 3.97	0.7401 ± 0.3600	3.28 ± 0.88	1.94 ± 0.51
CC	H	15.72 ± 1.41	50.96 ± 4.12	35.79 ± 6.28	2.0735 ± 0.6088	4.26 ± 0.35	2.51 ± 0.41
GC1	H	18.37 ± 1.26	57.77 ± 2.72	52.26 ± 6.45	3.3975 ± 0.6807	5.00 ± 0.36	2.76 ± 0.54
GC2	H	20.66 ± 1.88	64.48 ± 5.24	80.22 ± 14.21	4.9850 ± 1.3500	5.47 ± 0.55	3.41 ± 0.64

2016). In these animals, the AGs release the IAG hormone responsible for sexual differentiation and morphotypic determination, and the development of sexual characters. Its functionality has been demonstrated by silencing IAG gene expression with RNA interference (RNAi), promoting the inhibition of growth and also the development of secondary sexual characters in males of *M. rosenbergii* (Ventura et al., 2011a). Recently, intersexuality in the species studied here was attributed to hormonal disruption and a possible error in IAG expression, since *M. amazonicum* is a strictly gonochoric species (Paschoal and Zara, 2017).

The AG cells of *M. amazonicum* show two stages of secretory activity and secrete hormone of protein nature. In submissive morphotypes (TC and CC), the AGs are mainly composed of stage I cells – compact and

Table 3
Relationship between androgenic gland area (AG) and morphometric variables of *M. amazonicum* morphotypes and all males pooled. *a*: y-intercept; Al: allometry; *b:* slope; *CC*: cinnamon claw; CL: carapace length; *e*: eniantometry; GC1: green claw 1; GC2: green claw 2; MCL: major cheliped length; r^2: coefficient of determination; TC: translucid claw; TL: total length; * statistically significant at $p < 0.001$.

Relationship	Morphotypes	*b*	*a*	r^2	*t* (*b* = 1)	Al
AG *vs.* CL	TC	0.05	0.03	0.64	66.06*	–
	CC	−0.02	1.05	0.06	30.28*	*e*
	GC1	0.07	0.41	0.06	9.23*	–
	GC2	0.03	0.22	0.10	28.75*	–
	Pooled males	0.04	0.12	0.45	137.71*	–
AG *vs.* TL	TC	0.02	0.05	0.53	21.49*	–
	CC	−0.01	1.47	0.17	12.53*	*e*
	GC1	0.01	0.17	0.05	5.46*	–
	GC2	0.02	0.35	0.22	9.44*	–
	Pooled males	0.01	0.06	0.44	42.89*	–
AG *vs.* MCL	TC	0.03	0.04	0.43	8.23*	–
	CC	−0.01	0.71	0.01	10.81*	*e*
	GC1	0.01	0.68	0.14	16.91*	–
	GC2	0.01	0.69	0.08	27.56*	–
	Pooled males	0.01	0.53	0.40	96.43*	–

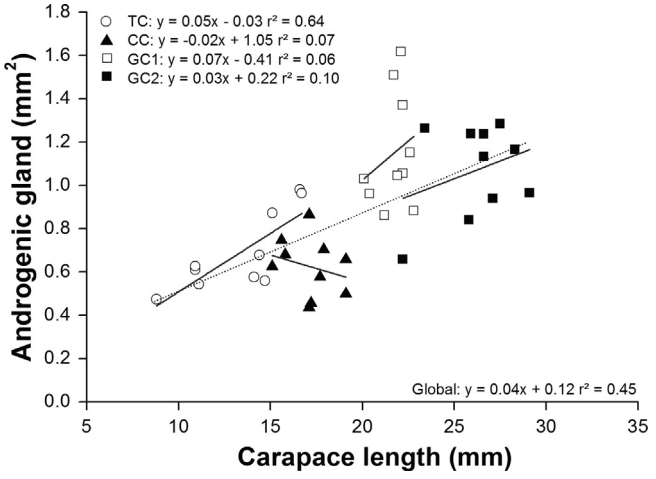

Fig. 5. Relationship between the androgenic gland area and carapace length for each morphotype (solid lines) and grouped males (Global: dotted line) of *M. amazonicum*. CC: cinnamon claw morphotype; GC1: green claw 1 morphotype; GC2: green claw 2 morphotype; r^2: coefficient of determination; TC: translucid claw morphotype.

without vacuolization, while in dominant morphotypes (GC1 and GC2), stage II cells were predominant and show vacuolated areas. However, the histochemical patterns of the cell stages were identical, showing a positive reactivity only for proteins. The difference between the stages is due to the displacement of cellular components after the dilation of RER at the beginning of stage II. These results show that the different stages of histological development of AGs are related to accumulation and secretion as proposed by Hoffman (1969) and Taketomi (1986), instead of distinct cell types with different functions, as suggested by Okumura and Hara (2004) and Phoungpetchara et al. (2011). Histochemical and ultrastructural patterns similar to those observed in *M. amazonicum* were verified in the AG cells of *M. rosenbergii* (Awari and Dube, 1999; Joseph, 2002; Okumura and Hara, 2004; Phoungpetchara et al., 2011). In this Indo-Pacific species, the androgenic hormone is composed of polypeptides with low-molecular-weight (16–18 kd – Sun et al., 2000), which confers positive results for histochemical tests for proteins in AG cells. The ultrastructural aspects of these cells demonstrate the protein nature of the AG hormone as firstly suggested by King (1964). The author verified a large abundance of highly dilated RER in the Lined shore crab *Pachygrapsus crassipes* (Randall, 1840), relating this ultrastructural pattern to protein-producing cells in vertebrates (e.g. endocrine pancreatic cells). Our results show that AG cells in *M. amazonicum* have typical characteristics of cells that synthesize proteins in a short period of time and store their products inside the dilated cisternae of RER when they are not immediately secreted, similar to plasma cells (Junqueira and Carneiro, 2008) or fat body cells in insects (Locke, 1984). This pattern of production and storage is similar to that found in other carideans, as well as in isopods, crayfishs and crabs (King, 1964; Radu and Crăciun, 1976; Taketomi et al., 1990; Martin et al., 1996; Phoungpetchara et al., 2011).

In *M. amazonicum*, secretion of the androgenic hormone probably occurs after cell degeneration and appears to us that a holocrine process is occurring. During the secretion, the AG cells and their organelles (specially the RER) become hypertrophied, followed by release and emission of the cellular content to hemolymph (evidencing by the strong vacuolization of the cytoplasm). Androgenic glands seem to us do not produce secretory granules of Golgian origin that accumulates in the cytoplasm. The absence of secretory products in AGs seems to be a rule in crustaceans (King, 1964; Hoffman; 1969; Radu and Crăciun, 1976; Martin et al., 1996). King (1964) demonstrated that the electron-dense bodies (up to 4 μm) are lysosomes, since he detected acid phosphatase activity in these structures. We also find these electron-dense bodies in the AGs of *M. amazonicum* and we speculate that they are lysosomes, but a future enzymatic essay is needed. These cellular components show variable structural aspects and accumulate acid hydrolases (Luzio et al., 2007). However, the function of this organelle in crustaceans AG is not yet fully understood, and could be associated with cell degeneration. Hoffman (1969) suggested that lysosomes release autolytic enzymes as soon as the AG cells begin to degenerate. Radu and Crăciun (1976) studying the terrestrial isopod *Porcellio scaber* Latreille, 1804 raised that when the cell is altered during the process of hypertrophy, the regeneration becomes impossible to be performed. Consequently, the degeneration becomes irreversible, leading to cell destruction and release of the cellular content to hemolymph, i.e. holocrine gland.

The AGs in initial (TC) and dominant morphotypes (GC1 and GC2) of *M. amazonicum* increase as the animal grows and are larger in the GC1 morphotype, whereas in the intermediate morphotype (CC) the AGs tend to decrease, i.e. an eniantometric process (*sensu* Teissier, 1960). In *Macrobrachium* prawns, the hypertrophy of the chelipeds is modulated by the AGs, being the AG activity higher in dominant morphotypes (Nagamine et al., 1980a,b; Okumura and Hara, 2004; Ventura et al., 2011b). Male prawns of *M. amazonicum* tend to invest much energy to develop large chelipeds (i.e. sexual weapons), increasing the fitness in intraspecific competitions (Augusto and Valenti, 2016; Paschoal and Zara, 2018, 2019). Recently, Pantaleão et al. (2014) and Paschoal and Zara (2019) recorded a positive allometry for major cheliped length (MCL) only in GC1 morphotype (Table 1). The latter authors suggest that GC1 males accumulate much energy for the development of robust sexual weapons during their passage to the GC2 morphotype. This may explain the large amplitude and higher values of the AGs area registered for GC1 males. The smaller size of the AGs registered for the GC2 morphotype corroborates this point, once the somatic growth of this morphotype is interrupted shortly after its passage from GC1 to GC2. Also, the energy accumulated by CG2 male is destined to the maintenance of metabolic processes, instead of maintenance of sexual weapons and sperm production (Moraes-Riodades and Valenti, 2004; Augusto and Valenti, 2016; Paschoal and Zara, 2018). On the other hand, the decrease of the AGs area in the intermediate morphotype CC may be related to a “reproductive diapause” during the sequential development of morphotypes. The seminiferous tubules of the testes of CC males are nearly or completely filled by spermatocytes, i.e. spermiogenesis does not or rarely occurs in this morphotype (Papa, 2007; Silva et al., 2009; Paschoal and Zara, 2019). In addition, CC males show high values of hepatosomatic index, near to those recorded for the dominant morphotypes (Paschoal, 2017). This

pattern is probably due to a lower AG activity in this morphotype, similar to that occurring in the intermediate morphotype of *M. rosenbergii* and may be common in carideans with social hierarchy in their population (Sagi et al., 1988; Joseph and Kurup, 2001; Ventura et al., 2011b). Commonly, intermediate morphotype prawns accumulate energy to become sexually active dominant males with large quantity of spermatozoa in their testes and VD (Sagi et al., 1988; Silva et al., 2009; Paschoal, 2017).

Despite the different life histories recorded for *M. amazonicum*, there are no differences in anatomical and histological aspects of AGs for populations analyzed (i.e. highly conservative pattern). The AGs in males have similar histochemical and ultrastructural patterns along the sequential development of morphotypes. However, the size of these structures change as they pass from one morphotype to another and this is directly related to the type of reproductive strategy adopted by each morphotype: energy and spermatocyte accumulation in the intermediate morphotype, and development of sexual weapons in dominant morphotypes. The information of the present study can be used in the maintenance of breeders and improvement of stocks, and also in future studies involving sexual manipulation and reversion in *M. amazonicum*. Due to the absence of differences in AGs patterns for hololimnetic and amphidromous populations of the Amazon River prawn, we suggest the investigation of the potential of hololimnetic prawns for aquaculture, as they do not depend on salt water as the amphidromous farmed populations. Thus, the farming and rearing of hololimnetic populations could be easier to manage, reducing the costs of production. The mechanisms of hormone production, accumulation and release and the function of lysosomes in AGs of crustaceans are still uncertain. Thus, future studies focusing exclusively on the secretory pathways of these glands are necessary to fill this gap.

5. Conclusions

Male prawns of *M. amazonicum* do not show any differences in the morphological, histochemical and ultrastructural patterns of the AGs between the amphidromous and hololimnetic populations. Male submissive morphotypes (TC and CC) have small AGs concentrated in the bulbs of the ejaculatory ducts, while in dominant morphotypes (GC1 and GC2) these glands are large and spread over the vasa diferentia. The AGs are composed by two cell stages (both stages positive only for proteins), being the stage I cells more common in submissive morphotypes, while stage II cells predominated in dominant morphotypes. Stage I cells show the cytoplasm nearly completely filled by RER with numerous parallel cisternae, without vacuoles. The RER in stage II cells is highly dilated, with distended cisternae (full of thin granular material) forming vacuoles. Hormone release in this species probably occurs by holocrine secretion. In CC males, AGs size decreases as the animal grows ("reproductive diapause"), while at the other three morphotypes AGs size increases as the prawn grows. This integrative approach provides a better comprehension of the androgenic gland of the species, helping researchers and producers/farmers to perform and conduct studies involving sexual manipulation and reversion, and improve breeding programmes and quality of stocks. This information is necessary to ensure a sustainable exploitation of the fishery resource.

Acknowledgements

This study was financed in part by the Coordenação de Aperfeiçoamento de Pessoal de Nível Superior – Brasil (CAPES) – Finance Code 001. FJZ thanks CAPES Ciências do Mar CIMAR II #1989/2014 proc. 23018.004309/2014-5 and São Paulo Research Foundation FAPESP (Biota #2010/50188-8). We thank Dr. Fernando L.M. Mantelatto, Dr. Rogério C. Costa and Dr. João F. Pantaleão for the constructive reviews and suggestions during the PhD committee. We especially thank Dr. Abner Carvalho Batista for provide an important insight about the growth (eniantometric) process. This study carried out according to Brazilian laws (MMA-ICMbio, license 47653-1 to LRPP, and MMA-ICMbio, permanent license 34587-1 to FJZ).

Appendix A. Supplementary data

Supplementary data to this article can be found online at https://doi.org/10.1016/j.ygcen.2019.01.014.

References

Augusto, A., Valenti, W.C., 2016. Are there any physiological differences between the male morphotypes of the freshwater shrimp *Macrobrachium amazonicum* (Heller, 1862) (Caridea: Palaemonidae)? J. Crust. Biol. 36, 716–723.
Awari, S.A., Dube, K., 1999. Histological and histochemical study of the androgenic gland of *Macrobrachium rosenbergii* (De Man). J. Aquacult. Trop. 14, 101–112.
Bortolini, J.L., Bauer, R.T., 2016. Persistence of reduced androgenic glands after protandric sex change suggests a basis for simultaneous hermaphroditism in a caridean shrimp. Biol. Bull. 230, 110–119.
Charniaux-Cotton, H., 1954. Découverte chez un crustacé amphipode (*Orchestia gamarella*) d'une glande endocrine responsible de la différenciation des caractères sexuels primaries et secondaires males. Comptes Rendus Acad. Sci. 239, 780–782.
Charniaux-Cotton, H., 1958. Contrôle hormonal de la différenciation du sexe et de la reproduction chez lês crustacés supérieurs. Bull. Soc. Zool. Fr. 83, 314–336.
Correa, C., Thiel, M., 2003. Mating systems in caridean shrimp (Decapoda: Caridea) and their evolutionary consequences for sexual dimorphism and reproductive biology. Rev. Chil. Hist. Nat. 76, 187–203.
Correa, C., Baeza, J.A., Hinojosa, I.A., Thiel, M., 2003. Male dominance hierarchy and mating tactics in the rock shrimp *Rhynchocinetes typus* (Decapoda: Caridea). J. Crust. Biol. 23, 33–45.
Gotelli, N.J., Ellison, A.M., 2004. A Primer of Ecological Statistics, first ed. Sinauer Associates, Inc., Sunderland, Massachusetts.
Gould, S.J., 1966. Allometry and size in ontogeny and phylogeny. Biol. Rev. Camb. Philos. Soc. 41, 587–638.
Hoffman, D.L., 1969. The development of the androgenic glands of a protandric shrimp. Biol. Bull. 137, 286–296.
Joseph, A., 2002. Histological, histochemical and biochemical characterization of male morphotypes of *Macrobrachium rosenbergii* (De Man) (PhD thesis). Cochin University of Science and Technology, Cochin, India, pp. 212.
Joseph, A., Kurup, B.M., 2001. Histological characterization of male morphotypes of *Macrobrachium rosenbergii* (de Man). In: Boopendrnath, M.R., Meenakumari, B., Joseph, J., Sankar, T.V., Praveen, P., Edwin, L. (Eds.), Riverine and Reservoir Fisheries of India. Society of Fisheries Technologists, Cochin, India, pp. 245–255.
Junqueira, L.C.U., Junqueira, L.M.M.S., 1983. Técnicas Básicas de Citologia e Histologia, first ed. São Paulo, Santos.
Junqueira, L.C.U., Carneiro, J., 2008. Histologia básica, eleventh ed. Ed. Guanabara Koogan, Rio de Janeiro.
Karplus, I., Barki, A., 2018. Male morphotypes and alternative mating tactics in freshwater prawns of the genus *Macrobrachium*: a review. Rev. Aquac. 1–16.
Kuris, A.M., Ra'anan, Z., Sagi, A., Cohen, D., 1987. Morphotypic differentiation of male Malaysian prawns, *Macrobrachium rosenbergii*. J. Crust. Biol. 7, 219–237.
Langer, S., Chalotra, R., Kour, T., 2002. The occurrence and description of male morphotypes of *Macrobrachium dayanum*. J. Anim. Physiol. Anim. Nutr. 49, 49–54.
Locke, M., 1984. The structure and development of the vacuolar system in the fat body of insects. In: King, R.C., Akai, H. (Eds.), Insect Ultrastructure. Springer, Boston, pp. 151–197.
Luzio, J.P., Pryor, P.R., Bright, N.A., 2007. Lysosomes: fusion and function. Nat. Rev. Mol. Cell Biol. 8, 622–632.
Maciel, C.R., Valenti, W.C., 2009. Biology, fisheries, and aquaculture of the Amazon River prawn *Macrobrachium amazonicum*: a review. Nauplius 17, 61–79.
Martin, G., Raimond, R., Laulier, M., Juchault, P., 1996. Ultrastructural and experimental studies on the androgenic gland in juvenile and puberal males of *Sphaeroma serratum* (Isopoda, Flabellifera). Crustaceana 69, 349–358.
Mello, M.L.S., Vidal, B.C., 1980. Práticas de Biologia Celular, first ed. Funcamp, Campinas.
Moraes-Riodades, P.M.C., Valenti, W.C., 2004. Morphotypes in male Amazon river prawns, *Macrobrachium amazonicum*. Aquaculture 236, 297–307.
Moraes-Valenti, P.M., Valenti, W.C., 2010. Culture of the Amazon River prawn *Macrobrachium amazonicum*. In: New, M.B., Valenti, W.C., Tidwell, J.H., D'ABramo, L.R., Kutty, M.N. (Eds.), Freshwater Prawns: Biology and Farming. Wiley-Blackwell, Oxford, England, pp. 485–501.
Nagamine, C., Knight, A.W., Maggenti, A., Paxman, G., 1980a. Effects of androgenic gland ablation on male primary and secondary sexual characteristics in the Malaysian prawn, *Macrobrachium rosenbergii* (de Man) (Decapoda, Palaemonidae), with first evidence of induced feminization in a nonhermaphroditic decapod. Gen. Comp. Endocrinol. 41, 423–441.
Nagamine, C., Knight, A.W., Maggenti, A., Paxman, G., 1980b. Masculinization of female *Macrobrachium rosenbergii* (de Man) (Decapoda, Palaemonidae) by androgenic gland implantation. Gen. Comp. Endocrinol. 41, 442–457.
New, M.B., 2005. Freshwater prawn farming: global status, recent research and a glance at the future. Aquacult. Res. 36, 210–230.
Okumura, T., Hara, M., 2004. Androgenic gland cell structure and spermatogenesis during the molt cycle and correlation to morphotypic differentiation in the giant freshwater prawn, *Macrobrachium rosenbergii*. Zool. Sci. 21, 621–628.

Pantaleão, J.A.F., Hirose, G.L., Costa, R.C., 2014. Ocurrence of male morphotypes of *Macrobrachium amazonicum* (Caridea, Palaemonidae) in a population with an entirely freshwater life cycle. Braz. J. Biol. 74, 223–232.

Papa, L.P., 2007. (PhD thesis) In: Caracterização estrutural do sistema reprodutor masculino e do hepatopâncreas dos diferentes morfótipos de *Macrobrachium amazonicum*. Universidade Estadual Paulista – UNESP Jabotical, São Paulo, Brazil, pp. 94.

Paschoal, L.R.P., 2017. (PhD thesis) In: História natural de *Macrobrachium amazonicum* (Heller, 1862) (Decapoda: Palaemonidae) e sua importância em reservatórios neotropicais do sudeste brasileiro. Universidade Estadual Paulista – UNESP Rio Claro, São Paulo, Brazil, pp. 320.

Paschoal, L.R.P., Zara, F.J., 2017. First record of intersexuality in the Amazon River shrimp *Macrobrachium amazonicum* (Heller, 1862) (Caridea: Palaemonidae). J. Crust. Biol. 37, 507–511.

Paschoal, L.R.P., Zara, F.J., 2018. Sperm count of *Macrobrachium amazonicum* (Heller, 1862) populations with distinct life histories, with introduction of a simple counting method. Aquaculture 491, 368–374.

Paschoal, L.R.P., Zara, F.J., 2019. Size at onset of sexual maturity in *Macrobrachium amazonicum* (Heller, 1862) phenotypes: an integrative approach. An. Acad. Bras Ciênc. 91 (3) in press.

Pearse, A.G.E., 1960. Histochemistry: Theoretical and Applied, first ed. J&A Churchill, London.

Phoungpetchara, I., Tinikul, Y., Poljaroen, J., Chotwiwatthanakun, C., Vanichviriyakit, R., Sroyraya, M., Hanna, P.J., Sobhon, P., 2011. Cells producing insulin-like androgenic gland hormone of the giant freshwater prawn, *Macrobrachium rosenbergii*, proliferate following bilateral eyestalk-ablation. Tissue Cell 43, 165–177.

Pileggi, L.G., Magalhães, C., Bond-Buckup, G., Mantelatto, F.L., 2013. New records and extension of the known distribution of some freshwater shrimps in Brazil. Rev. Mex. Biodivers. 84, 563–574.

Prakash, S., Ajithkumar, T.T., Bauer, R., Thiel, M., Subramoniam, T., 2016. Reproductive morphology and mating behaviour in the hingebeak shrimp *Rhynchocinetes durbanensis* Gordon, 1936 (Decapoda: Caridea: Rhynchocinetidae) in India. J. Mar. Biol. Assoc. U.K. 96, 1331–1340.

R CORE TEAM, 2016. R (The R Project for Statistical Computing). Software version 3.3.1. https://www.r-project.org/ (accessed 01.12.16).

Ra'anan, Z., Sagi, A., 1985. Alternative mating strategies in male morphotypes of the freshwater prawn *Macrobrachium rosenbergii* (De Man). Biol. Bull. 169, 592–601.

Radu, V.Gh., Crăciun, C., 1976. The ultrastructure of the androgenic gland in *Porcellio scaber* Latr. (terrestrial isopods). Cell Tissue Res. 175, 245–263.

Sagi, A., Aflalo, E.D., 2005. The androgenic gland and monosex culture of freshwater prawn *Macrobrachium rosenbergii* (De Man): a biotechnological perspective. Aquac. Res. 36, 231–237.

Sagi, A., Milner, Y., Cohen, D., 1988. Spermatogenesis and sperm storage in the testes of the behaviorally distinctive male morphotypes of *Macrobrachium rosenbergii* (Decapoda, Palaemonidae). Biol. Bull. 174, 330–336.

Sagi, A., Cohen, D., Milner, Y., 1990. Effect of androgenic gland ablation on morphotypic differentiation and sexual characteristics of male freshwater prawns, *Macrobrachium rosenbergii*. Gen. Comp. Endocrinol. 77, 15–22.

Sagi, A., Snir, E., Zimmermann, S., 1995. Efeitos da ablação da glândula androgênica no crescimento e na reversão sexual de machos do camarão de água doce *Macrobrachium rosenbergii* (De Man). R. Bras. Zootec. 24, 300–309.

Sagi, A., Snir, E., Khalaila, I., 1997. Sexual differentiation in decapod crustaceans: role of the androgenic gland. Invertebr. Repr. Dev. 31, 55–61.

Silva, G.M.F., Pantoja Ferreira, M.A., Von Ledebur, E.I.C.F., Da Rocha, R.M., 2009. Gonadal structure analysis of *Macrobrachium amazonicum* (Heller, 1862) from a wild population: a new insight into the morphotype characterization. Aquac. Res. 40, 798–803.

Soundarapandian, P., Dinakaran, G.K., Varadharajan, D., 2013. Alternative mating strategies in male morphotypes of the prawn *Macrobrachium idella idella* (Hilgendorf, 1898). J. Aquac. Res. Dev. 5, 1–10.

Sun, P.S., Weatherby, T.M., Dunlap, M.F., Arakaki, K.L., Zacarias, D.T., Malecha, S.R., 2000. Developmental changes in structure and polypeptide profile of the androgenic gland of the freshwater prawn *Macrobrachium rosenbergii*. Aquac. Int. 8, 327–334.

Taketomi, Y., 1986. Ultrastructure of the androgenic gland of the crayfish, *Procambarus clarki*. Cell Biol. Int. Rep. 10, 131–136.

Taketomi, Y., Murata, M., Miyawaki, M., 1990. Androgenic gland and secondary sexual characters in the crayfish *Procambarus clarkii*. J. Crust. Biol. 10, 492–497.

Teissier, G., 1960. Relative growth. In: Waterman, T.H. (Ed.), The Physiology of Crustacea, vol. 2. Metabolism and growth. Academic Press, New York, pp. 537–560.

Thiel, M., Chak, S.T.C., Dumont, C.P., 2010. Male morphotypes and mating behavior of the dancing shrimp *Rhynchocinetes brucei* (Decapoda: Caridea). J. Crust. Biol. 30, 580–588.

Ventura, T., Sagi, A., 2012. The insulin-like androgenic gland hormone in crustaceans: from a single gene silencing to a wide array of sexual manipulation-based biotechnologies. Biotechnol. Adv. 30, 1543–1550.

Ventura, T., Rosen, O., Sagi, A., 2011a. From the discovery of the crustacean androgenic gland to the insulin-like hormone in six decades. Gen. Comp. Endocrinol. 173, 381–388.

Ventura, T., Manor, R., Aflalo, E.D., Weil, S., Khalaila, I., Rosen, O., Sagi, A., 2011b. Expression of an androgenic gland-specific insulin-like peptide during the course of prawn sexual and morphotypic differentiation. ISRN Endocrinol. 2011, 1–11.

Zara, F.J., Toyama, M.H., Caetano, F.H., López-Greco, L.S., 2012. Spermatogenesis, spermatophore and seminal fluid production in the adult blue crab *Callinectes danae* (Portunidae). J. Crust. Biol. 32, 249–262.